In vitro cytotoxicity assessment of monocationic and dicationic pyridinium-based ionic liquids on HeLa, MCF-7, BGM and EA.hy926 cell lines

S. A. Pérez[1], *M. G. Montalbán*[2]*, *G. Carissimi*[1], *P. Licence*[3] *and G. Víllora*[1]

[1]Chemical Engineering Department, Faculty of Chemistry, Regional Campus of International Excellence "Campus Mare Nostrum", University of Murcia, 30071, Murcia, Spain.

[2]Chemical Engineering Department, University of Alicante, Apartado 99, 03080, Alicante, Spain.

[3]School of Chemistry, The University of Nottingham, University Park, Nottingham, UK.

*Corresponding author: mercedes.garciam@ua.es

Abstract

Dicationic ionic liquids (ILs) generally possess higher thermal and electrochemical stability than the analogous monocationic ILs, which makes them more suitable for high-temperature applications as solvents for organic reactions, lubricants or stationary phase in gas chromatography. However, knowledge on dicationic IL cytotoxicity is still scarce. Here we explore the cytotoxicity of twelve mono- and dicationic pyridinium-based ILs on HeLa, MCF-7, BGM and EA.hy926 cells. The 3-(4,5-dimethylthiazol-2-yl)-2,5-diphenyltetrazolium bromide (MTT) assay, cell cycle arrest assays, apoptosis experiments and orange staining were carried out. The results showed that dicationic ILs are generally less cytotoxic than their monocationic counterparts. In monocationic ILs, cytotoxicity was stronger when they contain long alkyl chains, because of their higher lipophilicity. However, the full effect of the length of the linkage alkyl chain of dicationic ILs on cytotoxicity is not clear probably because the chain is “trapped” between both cationic moieties. IL cytotoxicity is highly dependent on the cell type, and HeLa cells exposed to [C_{12}Pyr]Br die *via* apoptosis. The present study increases our knowledge of IL cytotoxicity on human and monkey cells and clarifies the cell death mechanism. The results suggest that dicationic ILs offer the potential to replace some monocationic ILs because of their lower cytotoxicity.

Keywords: Dicationic; ionic liquid; pyridinium; MTT assay; apoptosis.

1. Introduction

Ionic liquids (ILs) are molten salts at low temperature (around or below 100 ºC). Low melting points are possible because the asymmetry of their ionic structure and the dispersion of their charges result in reduced inter-ion interaction energies and decreased lattice enthalpy (ΔH_L) (Ranke et al., 2004). ILs are typically composed of an organic cation with a bulky charge-carrying head group (imidazolium, pyrrolidinium, pyridinium, piperidinium, *etc.*) and one or more alkyl side chains, and a counterion which may be organic or inorganic, for example Cl^-, Br^-, AcO^- or $[Tf_2N]^-$ (Wu et al., 2018). ILs have been widely studied in research activities and even incorporated into several industrial processes because of their exclusive combination of properties, which include negligible vapor pressure, non-flammability, wide liquid state temperature range, high thermal and chemical stability and high ionic conductivity (Alvarez-Guerra and Irabien, 2011; Diaz et al., 2018; Lee and Lin, 2014). On a fundamental level, the most remarkable feature of ILs is the possibility of modulating their physicochemical properties, including their hydrophobicity, viscosity, density or solubility and their biodegradability or toxicity, by means of the appropriate selection of the cationic and anionic constituents (Montalbán et al., 2015; Ventura et al., 2012), which means that they can be designed for a specific application (Viswanathan et al., 2006). Initially ILs were proposed as more benign solvents and candidates to replace conventional organic solvents (Earle and Seddon, 2002), but they have also found applications in other areas, where they can be used as reaction media (de Los Ríos et al., 2007), catalysts (Welton, 2004), extraction agents (Montalbán et al., 2018a, 2016a) or supported liquid membranes (Hernández-Fernández et al., 2008, 2007), and in lithium ion batteries (Balducci, 2017), dye-sensitized solar cells (Denizalti et al., 2018) or the synthesis of biopolymeric nanoparticles (Lozano-Pérez et al., 2015).

Dicationic ILs are an interesting sub-class of materials that can be easily prepared by the functionalization of a central linker fragment with two discrete cationic charge carriers (Montalbán et al., 2018b; Steudte et al., 2014). Compared to monocationic ILs, dicationic ILs may possess even higher thermal and moderately increased electrochemical stability, making

them more suitable for use in high-temperature applications as solvents for reactions (Han and Armstrong, 2005), lubricants (Jin et al., 2006) or as stationary phases in gas chromatography (Qi and Armstrong, 2007). Because ILs are widely used in academic research and have potential use in industry, more studies related to their toxicity are required since they may enter to the living environment and the risks associated with them are still far from being known in any depth (Wu et al., 2018), especially in the case of the more recently discovered dicationic ILs. As mentioned above, the release of ILs into the atmosphere is difficult because they are not volatile (Gómez-Herrero et al., 2018). However, a great number of ILs (all those which are hydrophilic), are notably soluble in water and hence bioavailable so they can easily enter water streams or soils (Diaz et al., 2018; Montalbán et al., 2016b) with serious effects on human health and the environment. By contrast, ILs which contain a hydrophobic anion (PF_6^-, Tf_2N^-, among others) are practically non-soluble in water and have poor bioavailability. ILs with halogen anions (chloride, bromide or iodide), such as the ILs studied in this work, are highly hydrophilic and extremely water soluble, with a high degree of bioavailability (Huddleston et al., 2001). Given the wide potential use of mono- and dicationic ILs in industrial processes, especially as an alternative to conventional solvents, and their possible release into the environment by accidental spills or as residues, analysis of their toxicological fate is imperative. In addition, some ILs have recently been seen to be of interest in the biological and pharmaceutical field as platforms to overcome problems associated with new drugs, such as their low solubility in water and poor bioavailability (Egorova et al., 2017; Vieira et al., 2019). To this end, several studies have reported that ILs are able to increase the water solubility of poorly soluble drugs because of their capacity for dissolving pharmaceutical ingredients and for acting as drug reservoirs in controlled release devices (Mahkam et al., 2016; Miwa et al., 2016; Mizuuchi et al., 2008; Moniruzzaman et al., 2010). New dicationic imidazolium-based ILs have recently been synthesized and their potential use as antimicrobial materials has been demonstrated (Gindri et al., 2014). These recent applications of ILs make the study of their biocompatibility and cytotoxicity even more necessary.

Studies related to the toxicity of dicationic ILs are very scarce in the literature. e Silva et al. (2014) studied the (eco)toxicity of dicationic cholinum-based ILs in *Vibrio fischeri* on the basis of the luminescence inhibition of this bacterium. Steudte et al. (2014) used several toxicity tests of different levels of biological complexity to study a group of dicationic imidazolium and pyrrolidinium-based ILs. They used enzyme inhibition tests (acetylcholinesterase), algae (*Scenedesmus vacuolatus*), fish (*Daphnia magna*) and cell lines (IPC-81) to carry out the experiments. Gindri et al. (2014) screened the cytotoxicity of a set of dicationic imidazolium-based ILs on MC3T3-E1 pre-osteoblast cells.

In this study, we evaluate the cytotoxicity of 10 pyridinium-based ILs (5 dicationic ILs and their monocationic counterparts) on four cell lines: Human cervical cancer cells (HeLa), Human breast cancer cells (MCF-7), green monkey kidney epithelial cells (BGM) and human umbilical immortalized cells (EA.hy926). A comparison between the cytotoxicity of dicationic and monocationic ILs is carried out in order to study the influence of the dicationic moiety structure, while the effect of the alkyl chain length and cell line on cytotoxicity in both groups of ILs is also analyzed. To the best of our knowledge, this is the first time that the cytotoxicity of these dicationic ILs has been measured.

2. Material and Methods

2.1. Ionic liquids

The full name and chemical structure of the ILs used are presented in Table 1. The monocationic ILs [C_2Pyr]Br (purity>99%), [C_4Pyr]Br (purity>99%), [C_6Pyr]Br (purity>99%), [C_8Pyr]Br (purity>99%) and [C_{12}Pyr]Br (purity>99%) were purchased from IoLiTec (Germany). The dicationic ILs used in this study ([C_2(Pyr)$_2$]Br_2, [C_4(Pyr)$_2$]Br_2, [C_6(Pyr)$_2$]Br_2, [C_8(Pyr)$_2$]Br_2 and [C_{12}(Pyr)$_2$]Br_2) were synthesized and characterized as described in previous papers (Montalbán et al., 2018b; Montalbán et al., 2018c).

Table 1. Abbreviations, full names and chemical structures of the studied ILs.

IL abbreviation	IL full name	Cation	Anion
$[C_2Pyr]Br$	1-ethylpyridinium bromide	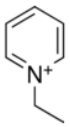	Br^-
$[C_4Pyr]Br$	1-butylpyridinium bromide	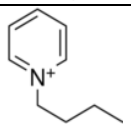	Br^-
$[C_6Pyr]Br$	1-hexylpyridinium bromide	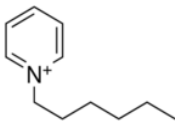	Br^-
$[C_8Pyr]Br$	1-octylpyridinium bromide	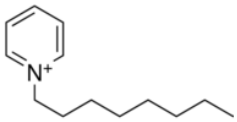	Br^-
$[C_{12}Pyr]Br$	1-dodecylpyridinium bromide	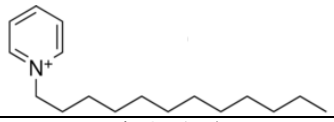	Br^-
$[C_2(Pyr)_2]Br_2$	1,2-bis(pyridinium-1-yl)ethane dibromide	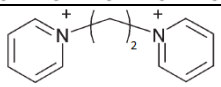	$2Br^-$
$[C_4(Pyr)_2]Br_2$	1,4-bis(pyridinium-1-yl)butane dibromide	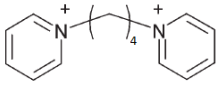	$2Br^-$
$[C_6(Pyr)_2]Br_2$	1,6-bis(pyridinium-1-yl)hexane dibromide	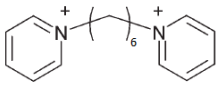	$2Br^-$
$[C_8(Pyr)_2]Br_2$	1,8-bis(pyridinium-1-yl)octane dibromide	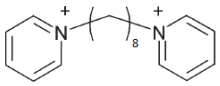	$2Br^-$
$[C_{12}(Pyr)_2]Br_2$	1,12-bis(pyridinium-1-yl)dodecane dibromide	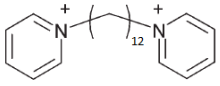	$2Br^-$

2.2. Cell lines and culture media

Human cervical cancer cells (HeLa), Human breast cancer cells (MCF-7), green monkey kidney epithelial cells (BGM) and human umbilical immortalized cells (EA.hy926) were acquired from the American Type Tissue Culture Collection (ATCC, USA). Cell lines were maintained in Dulbecco's Modified Eagle Medium (DMEM) with a low glucose content (1 g/L) supplemented with 10% (v/v) fetal bovine serum (FBS), 1 mM glutamax, 1 % antibiotics (penicillin-streptomycin) and 1 mM pyruvate. In all cases, cells were maintained at 37ºC in 5% CO_2 with 95% humidity atmosphere. Cells were sub-cultured and the medium was changed once a week. In all cases, 0.25% trypsine-0.25 mM ethylenediaminetetraacetic acid (EDTA) were used. Before

and after the experiments, all cell lines were seen to be mycoplasma-free, as determined by the Hoechts DNA stain method (Chen, 1976).

2.3. Cytotoxicity assay

A total of 5×10^3 cells/well (150 µL of culture medium as described above) were seeded in a 96-well plate and incubated at 37 ºC in a 5% CO_2 and 95% humidity atmosphere for 24 h. The IL solutions were diluted in complete medium at 100 mM concentration for dicationic ILs and 250 µM for the monocationic ILs. The resulting solution was then diluted successively (1:1 dilutions) to obtain a total of 16 solutions of diminishing concentration. These dilutions differed depending on the IL in question and their cytotoxic effect on each cell line. The dilutions were added to each well at a final volume of 150 µL. Cells were incubated at 37 ºC for 48 h. The medium was then removed from the wells and 200 µL of MTT (3-(4,5-dimethylthiazol-2-yl)-2,5-diphenyltetrazolium bromide, 1 mg/mL final concentration) was added. After 4 h incubation in identical conditions, MTT was removed and 100 µL of dimethyl sulfoxide (DMSO) was added. The absorbance at 560 nm was then recorded on a Fluostar Omega spectrophotometer.

The absorbance at each compound concentration was translated into inhibition percentage, *I*%, according to the following equation,

$$I\% = \left[1 - \frac{A_T}{A_C}\right] x100 \qquad [1]$$

where A_T and A_C are the absorbances of treated and control cells, respectively.

IC_{50} values were obtained from a three parameter fitting of the semi-logarithmic curves (*I*% as a function of the logarithm of the IL concentration) according to equation 2.

$$I\% = \frac{Imax}{1 + \left(\frac{IC_{50}}{C}\right)^n} \qquad [2]$$

where I_{max} is the maximum inhibition observed, IC_{50} is the IL concentration at which 50% of the cell population is dead, *C* is the IL concentration at which the inhibition *I*% is observed and *n* is

the slope of the curve at the IC_{50} value. The fitting was performed using GraphPad Prism v.6 software. All compounds were tested in three independent sets with triplicate points. The *in vitro* studies were performed in the SACE service with Level 2 Biosecurity (Support Service for Experimental Sciences, University of Murcia, Murcia, Spain).

2.4. Cell Cycle Arrest Assays

A total of 7.5×10^4 HeLa cells were seeded in 12-well plates and left at 37°C in a 5% CO_2 and 95% humidity atmosphere for 24 h. Monocationic or dicationic ILs with C_{12} chain used at the approximate IC_{50} concentration were then added to each well. Cells were incubated for 24 h and then removed from the wells with trypsin-EDTA, collected and centrifuged (200*g*, 5 min). The supernatant was removed and the cells were washed with phosphate-buffered saline (PBS) and centrifuged (200*g*, 5 min). The supernatant was also removed, and the cells were treated with ethanol (EtOH) at 70% (PBS, 30%) for 45 min at 4ºC. Finally, EtOH was removed by centrifugation. Cells were resuspended in 400 µL of PBS, and 50 µL RNase solution and 50 µL of propidium iodide (PI) were added at a final concentration of 0.1 mg/mL and 40 mg/mL, respectively. Cells were incubated for 30 min in the same conditions as for culture. The PI fluorescence was measured for each cell in a Becton-Dickinson FACScalibur flow cytometer. In each case 30000 events were acquired.

2.5. Apoptosis Experiments

To explore the cell death mechanism provoked by ILs, apoptosis experiments were performed. First, 7.5×10^4 of HeLa cells were typically seeded in a 12-well plate and maintained under normal culture conditions. After 24 h, the cells were treated with monocationic and dicationic ILs with C_{12} chain at the approximate IC_{50} concentration and incubated for a further 24 h. An apoptosis positive control with 8 µM camptotecin was used. Following incubation, media and cells were collected and centrifuged, the supernatant was discarded and cells were washed twice with PBS as described above (without the PBS/EtOH mix in this case). After removing the PBS, 40 µL of a solution containing Annexin V and PI (Annexin-V-Fluos from Roche) and 160 µL of incubation

buffer (Roche apoptosis kit) were added to the cell pellet. Cells were resuspended in this solution and left at room temperature in the dark for 15 min. 200 µL of PBS was added prior to determining the emission of PI and Annexin V at 620 and 525 nm, respectively. These measurements were carried out in a Becton-Dickinson FACScalibur flow cytometer. In each case, 10000 events were acquired.

2.6. Nuclei fluorescent imaging

Typically, $1{,}5x10^4$ HeLa cells were cultured in the same conditions as described above (DMEM supplemented, 37ºC, 5% CO_2 and 95-100% humidity) in a 4-well chamber slide system and left for 24 h. $[C_{12}Pyr]Br$ was then added at 8 µM and the cells in each individual well were fixed every 30 minutes with 70% alcohol and left in PBS buffer. Finally, a solution of 1ng/ml of acridine orange was added to each well, and the resulting cultures were incubated for 10 min. The resulting slide was observed under an inverted microscope (NIKON mod. Eclipse TE 2000U) for phase contrast and using a FITC filter for fluorescent images. Imaging cells were analyzed with ImageJ software. The statistical analysis was made with GraphPad Prims 6 software.

3. Results and Discussion

3.1. Cytotoxicity of mono- and dicationic pyridinium-based ILs

Carrying out *in vitro* cytotoxicity tests is important in the case of ILs and, especially when they are going to be used in biological and pharmaceutical applications and in other areas in which they could come into contact with humans, animals or the environment. The test is cost-effective, convenient and time saving (Vieira et al., 2019). IL cytotoxicity is greatly influenced by the chosen cell line and by IL structural features such as the cationic moiety, the length of the alkyl chain/s and the anion type (Wu et al., 2018). After exposing HeLa, MCF-7, BGM and EA.hy926 cells to a series of mono- and dicationic pyridinium-based ILs for 48 hours, IC_{50} values were calculated using a dose-response model, which was obtained from a sigmoidal fitting of dose-response curves as stated in *Section 2.3*. The calculated IC_{50} values are shown in Table 2. The corresponding dose-response curves of monocationic and dicationic ILs are represented in

194 Figures 1 and 2, respectively. It can be observed that the cytotoxicity of the ILs was dose-
195 dependent. The IC_{50} of $[C_{12}Pyr]Br$ on EA.hy926 cells was the lowest, with a value of 0.1 µM. By
196 contrast, the IC_{50} of $[C_4(Pyr)_2]Br_2$ on MCF-7 cells was the highest at 33.17 mM. From a
197 preliminary study of the results, we can infer that the IL cytotoxicity greatly depends on the IL
198 structure and on the cell line in question. As a general rule, the IC_{50} values obtained in this work
199 were high, reflecting the low cytotoxicity of the studied ILs and the probability that, at their
200 environmental concentration, they have no strong cytotoxic effect.

201 **Table 2.** IC_{50} values for HeLa, MCF-7, BGM and EA.hy926 cells exposed to mono- and
202 dicationic pyridinum-based ILs for 48 hours.

IL	IC_{50} (mM)			
	HeLa	MCF-7	BGM	EA.hy926
$[C_2Pyr]Br$	5.560±0.4307	26.300 ±5.8194	4.743±0.9068	6.511±0.4474
$[C_4Pyr]Br$	1.725 ±0.1771	6.439 ±0.8727	3.756 ±0.7244	1.998 ±0.2059
$[C_6Pyr]Br$	0.568±0.0707	3.262 ±0.5238	0.690±0.1487	0.228 ±0.03627
$[C_8Pyr]Br$	0.0159±0.0018	0.054±0.0047	0.211±0.0208	0.0007 ±0.0001
$[C_{12}Pyr]Br$	0.0046±0.0002	0.002±0.0002	0.018±0.0037	0.0001±0.00002
$[C_2(Pyr)_2]Br_2$	18.360 ± 0.529	6.553 ± 2.797	13.220 ± 0.529	22.100 ± 1.971
$[C_4(Pyr)_2]Br_2$	13.760 ± 1.218	33.170 ± 2.696	22.140 ± 0.336	19.560 ± 1.381
$[C_6(Pyr)_2]Br_2$	18.250 ± 0.641	17.410 ± 1.458	24.000 ± 1.033	8.428 ± 2.659
$[C_8(Pyr)_2]Br_2$	1.078 ± 0.141	6.979 ± 0.716	26.260 ± 0.249	0.408 ± 0.037
$[C_{12}(Pyr)_2]Br_2$	0.160 ± 0.030	0.529 ± 0.043	0.751 ± 0.066	0.008 ± 0.001

203

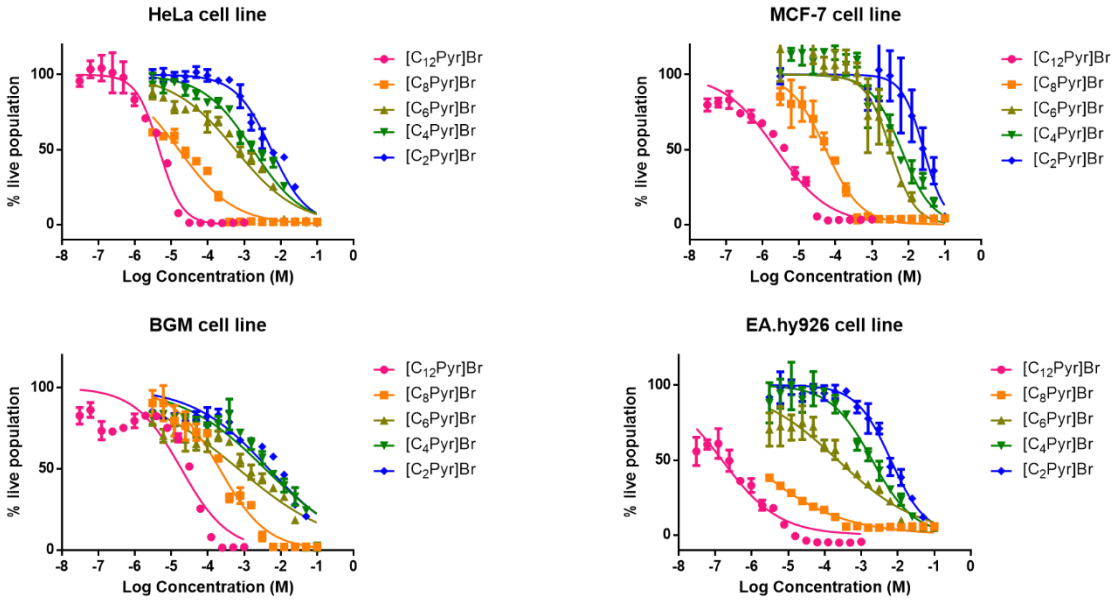

Figure 1. Dose-response curves of HeLa, MCF-7, BGM and EA.hy926 cells treated with five monocationic pyridinium-based ILs for 48 hours.

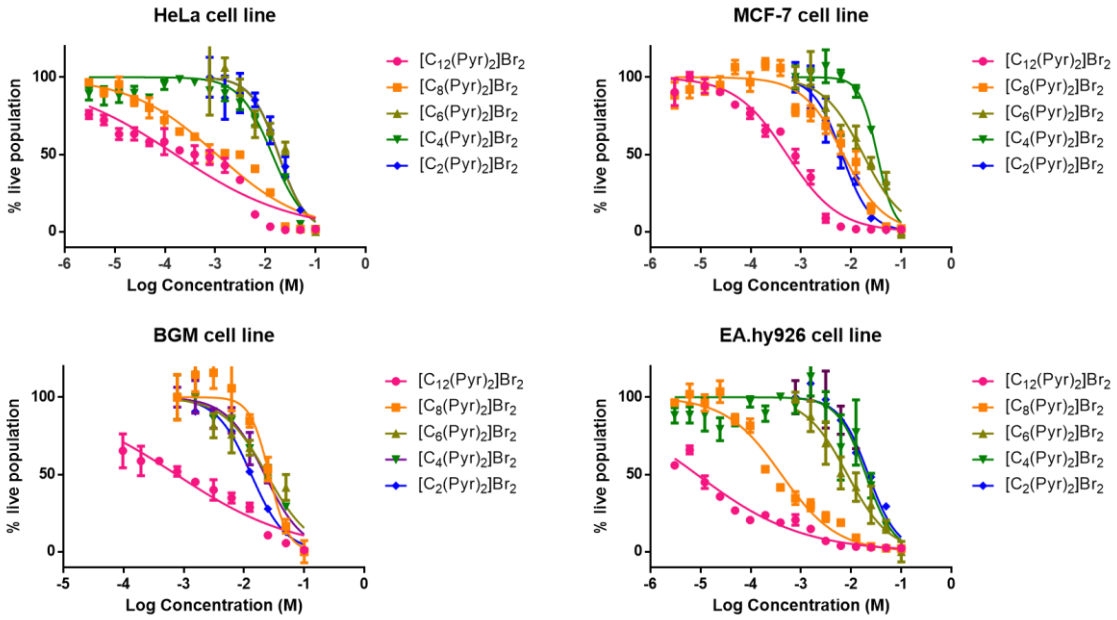

Figure 2. Dose-response curves of HeLa, MCF-7, BGM and EA.hy926 cells treated with five dicationic pyridinium-based ILs for 48 hours.

3.1.1. Monocationic *vs* dicationic ILs

To study the effect of the presence of one or two cationic moieties on the cytotoxicity of ILs, the cell viability of HeLa, MCF-7, BGM and EA.hy926 cells after treatment with five monocationic ILs and their five homologous dicationic ILs was evaluated. As can be seen in Figure 3, all the dicationic ILs studied showed higher IC_{50} values than their monocationic homologues, except $[C_2(Pyr)_2]Br_2$ on MCF-7 cells, and the difference was more pronounced as the alkyl chain length of the cation increased. These results agree with those of other authors, who observed that an additional cationic head reduced the IL toxicity compared with the corresponding monocationic IL (Gindri et al., 2014; Steudte et al., 2014). According to Gindri et al. (2014), in dicationic ILs, the alkyl chain, the length of which probably governs the cytotoxicity (McLaughlin et al., 2011), is masked between the two cationic moieties, losing its ability to interact with cell membranes and, therefore, reducing IL cytotoxicity. A similar conclusion was reached in IL (eco)toxicity studies (e Silva et al., 2014; Montalbán et al., 2018b). e Silva et al. (2014) suggested that the lower (eco)toxicity of dicationic ILs on *Vibrio fischeri* could be related to the bigger size of the molecules, which would hinder their interaction with the bacterial cell membranes. In addition, the second charge carrier stops the carbon chain, reducing the toxic potency (Montalbán et al., 2018b). This lower cytotoxicity of dicationic ILs constitutes an important advantage because it means that they can be specifically designed as alternatives to monocationic ILs, for biological and pharmaceutical applications in which their use is still limited.

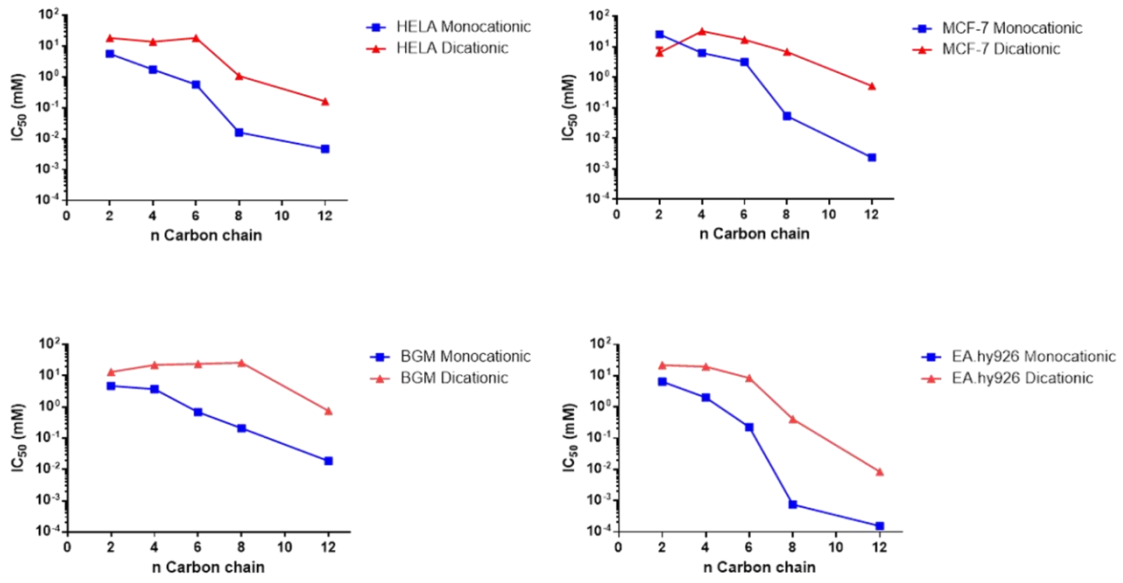

Figure 3. IC_{50} values for HeLa, MCF-7, BGM and EA.hy926 cells exposed to monocationic and dicationic pyridinium-based ILs with different alkyl chain lengths (the number of carbon atoms *n* ranged from C_2 to C_{12}) for 48 hours.

3.1.2. Influence of alkyl chain length

The cytotoxic effect of monocationic and dicationic pyridinium-based ILs with different alkyl chain lengths (number of carbon atoms n = 2, 4, 6, 8 and 12) on HeLa, MCF-7, BGM and EA.hy926 cells was studied. The results are shown in Figure 3. In the case of the monocationic ILs, their cytotoxicity on all the cell lines increased with the alkyl chain length as their IC_{50} values decreased. The link between increasing alkyl chain length and increasing cytotoxicity in monocationic ILs has been established in numerous studies (Li et al., 2012; McLaughlin et al., 2011; Steudte et al., 2014; Vieira et al., 2019; Wu et al., 2018). Lengthening of the alkyl chain of the cation is closely related to an increase in IL toxicity due to the increase of lipophilicity (Gal et al., 2012; Montalbán et al., 2016b). This increase in the lipophilic nature and the presence of delocalized charges would promote the disruption of the cell membrane and increase the internal acidity, with negative effects on cellular viability because of enzyme denaturation and oxidative stress (Gal et al., 2012; Vieira et al., 2019). According to Wu et al. (2018), the stronger the lipophilicity, the greater the possibility of contact with the lipid bilayer and hydrophobic proteins of the membrane, altering its normal physiological function and even leading to cell death.

As regards the dicationic ILs (Figure 3), a similar trend was found, but not so clear. With up to six carbon atoms in the alkyl chain, the IC_{50} of $[C_2(Pyr)_2]Br_2$, $[C_4(Pyr)_2]Br_2$ and $[C_6(Pyr)_2]Br_2$ on EA.hy926 and HeLa cells showed values of the same order of magnitude and, from $[C_8(Pyr)_2]Br_2$, cytotoxicity greatly increased. In BGM and MCF-7 cell lines, the IL cytotoxicity did not start to significantly increase until $[C_{12}(Pyr)_2]Br_2$. On the one hand, our results agree with other authors such as Gindri et al. (2014), who found that imidazolium-based dicationic ILs with different anions and cationic alkyl chains of 10 carbons were more toxic towards MC3T3-E1 pre-osteoblast cells than those with 8 carbons. On the other hand, the trend observed in this work was also found by Steudte et al. (2014) who reported that they did not observe the effect of greater toxicity on

promyelocytic leukemia rat cells (IPC-81) with increasing spacer length from 2 to 6 atoms of carbons in the studied dicationic ILs. However, they did find an effect when the length of the terminal side chains (not the linkage alkyl chain) increased from 1 to 5 atoms of carbons. The reason might be that, as stated before, the alkyl chain is "trapped" between the two cationic moieties and, although the hydrophobicity of the cation increases with the length of the linkage alkyl chain, the interaction of the alkyl chain with the cellular membrane is weaker and, consequently, cellular death is reduced.

3.1.3. Influence of cell type

In this study, the cell lines were selected due to their features and origin. Three of them (HeLa, MCF-7 and EA.hy926) were human cell lines and one of them (BGM) from monkey. HeLa cells are derived from cervical carcinoma and represent prototypical cells of the human epithelium. Epithelial cells were chosen because toxic compounds generally enter an organism through this site of first contact so they are a suitable model for studying IL cytotoxicity on human cells due to the direct contact (Stepnowski et al., 2004; Xia et al., 2018). MCF-7 cells are human breast cancer cells, which have been widely used in IL cytotoxicity studies because they are a well-characterized cell line (Kumar et al., 2008; Salminen et al., 2007). EA.hy926 cells coat the inside of blood vessels and are one of the most used and best characterized human vascular endothelial cell lines (Vieira et al., 2019). When ILs are used in pharmacological approaches with intravenous administration, the determination of IL cytotoxicity on endothelial vein cells such as EA.hy926 cells is of great value. BGM is a cell line of renal origin. It is a non-tumorigenic epithelial cell line which was chosen because it is a good reference to assess the toxicological effects of different compounds (Romero et al., 2004).

As can be seen in Figure 4 and Table 1, the IL cytotoxic effect is greatly influenced by the cell line, but the mechanism of IL cytotoxicity has not been fully elucidated yet. A similar conclusion was reached by other authors (Vieira et al., 2019). According to our results, it may be inferred that EA.hy926 cells are more sensitive to mono- or dicationic ILs with longer alkyl chains (C_6-

C_{12}), *i.e.* the most toxic of each series, while the cytotoxicity exhibited toward normal and cancer human cells is significantly different. For mono- or dicationic ILs with shorter alkyl chains (C_2-C_4), the cytotoxicity values are of the same order on all the cell lines and no trend can be established. The differences in the cellular viability of the different cell lines after exposure to the same IL could derive from the specific features and/or properties of the cells.

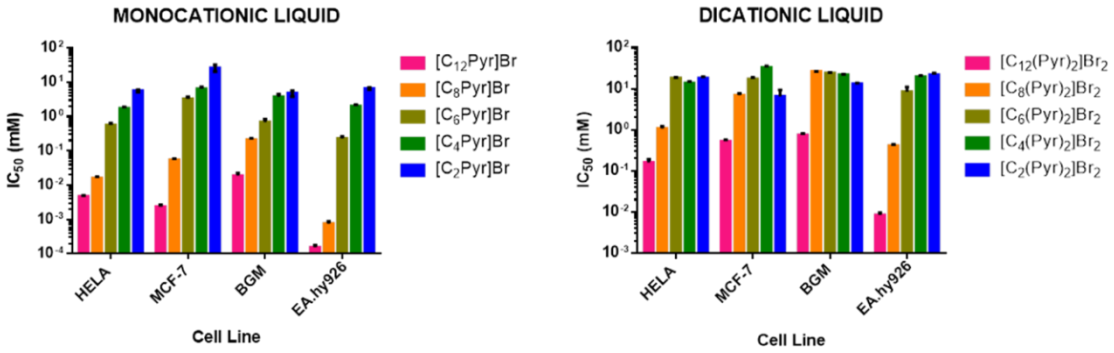

Figure 4. IC_{50} values for HeLa, MCF-7, BGM and EA.hy926 cells exposed to monocationic (left) and dicationic (right) pyridinium-based ILs for 48 hours.

3.2. Flow cytometry analysis of mono- and dicationic pyridinium-based ILs

For the flow cytometry analysis, HeLa cells were chosen as a model for their well-characterized cell cycle. As comparison between mono- and dicationic ILs, the assays were carried out with $[C_{12}Pyr]Br$ and $[C_{12}(Pyr)_2]Br_2$ since they are the most toxic ILs on HeLa cells in each series. The IC_{50} concentration of both ILs was chosen for the experiments.

3.2.1. Rate of apoptosis

To analyze the nature of cell death due to the effect of the ILs on HeLa cells, Annexin-V-Fluos Apoptosis Detection Kit was used to determine the rate of apoptosis provoked by 24 hours of treatment at the IC_{50} concentration of $[C_{12}Pyr]Br$ and $[C_{12}(Pyr)_2]Br_2$. The Annexin-V-Fluos stained graph consists of four quadrants (Q) where Q1 represents necrotic cells, Q2 and Q3 show late and early apoptotic cells, respectively and Q4 are the live cells. As negative control live HeLa cells which had not been treated with any IL were used, and the positive control, as mentioned in

Section 2.5, was HeLa cells treated with camptotecin, a chemical compound which induces cellular apoptosis. The positive control is normally used as comparison and, if similar results are found in the treated cells, it can be assumed that the cells have suffered apoptosis. As shown in Figure 5, the apoptotic effect in HeLa cells was dependent on the type of IL and its concentration. The apoptosis rate (Q2 + Q3) of the negative and positive controls was 19.82% and 56.9%, respectively. The apoptosis rate of the HeLa cells exposed to $[C_{12}Pyr]Br$ and $[C_{12}(Pyr)_2]Br_2$ at their IC_{50} concentration was 24.92% and 30.3%, respectively. As expected, these values are intermediate between both controls, indicating that the mechanism acting during cell death was mainly apoptotic. In addition, it could be inferred that early apoptosis and late apoptosis were the main cell death mechanisms for the monocationic and the dicationic IL, respectively. The results reveal that, to reach a similar rate of apoptosis, a considerably higher dicationic IL concentration was necessary, showing again its less cytotoxic behavior compared to its monocationic analogous.

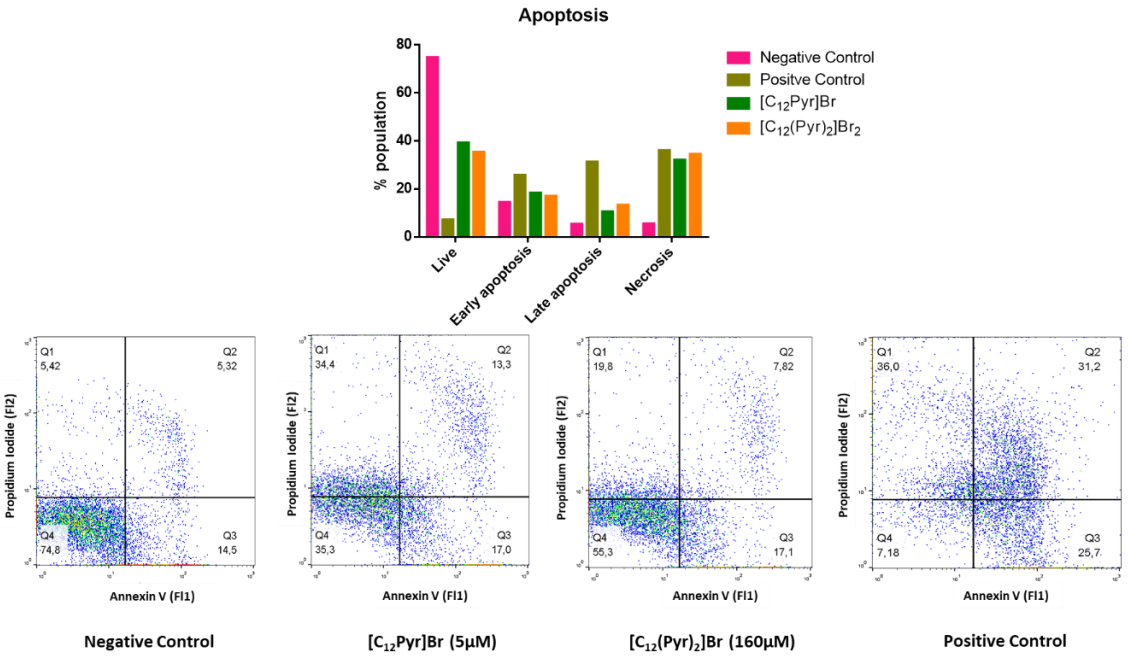

Figure 5. Flow cytometry analysis of apoptosis rate in HeLa cells after 24 hours of treatment with different concentrations of $[C_{12}Pyr]Br$ and $[C_{12}(Pyr)_2]Br_2$. HeLa cells not treated with IL were used as negative control and HeLa cells treated with camptotecin were used as positive control.

3.2.2. Influence of IL treatment on the cell cycle

The observed induction of apoptosis due to pyridinium-based IL treatment on HeLa cells further prompted us to study the inhibition mechanism of cell growth through cell cycle arrest by flow cytometric analysis. The cell cycle of HeLa cells exposed to $[C_{12}Pyr]Br$ and $[C_{12}(Pyr)_2]Br_2$ at the IC_{50} concentration for 24 hours was evaluated. According to Figure 6, the number of G1 phase cells slightly increased with respect to the control (unexposed cells) from 49.1% to 54.6 % and 53.5% when cells were exposed to $[C_{12}Pyr]Br$ and $[C_{12}(Pyr)_2]Br_2$, respectively. The number of cells in the S and G2/M phases decreased in both cases. The S cell number decreased from 27.7% to 23.4% and 24.5%, and the G2/M cell number from 16.6% to 13.1% and 13.3% with $[C_{12}Pyr]Br$ and $[C_{12}(Pyr)_2]Br_2$, respectively. Our results are in good agreement with previous IL cytotoxicity studies. Thamke et al. (2019) reported that another pyridinium-based monocationic IL, 1-butyl-4-methylpyridinium chloride, arrested animal cells (MDA-MB-231) in S and G2/M phases of the cell cycle. It can be concluded that the dicationic IL, $[C_{12}(Pyr)_2]Br_2$, is much less cytotoxic than the homologous monocationic IL, $[C_{12}Pyr]Br$, because a 32-fold concentration is necessary to have the same effect on the cell cycle of HeLa cells.

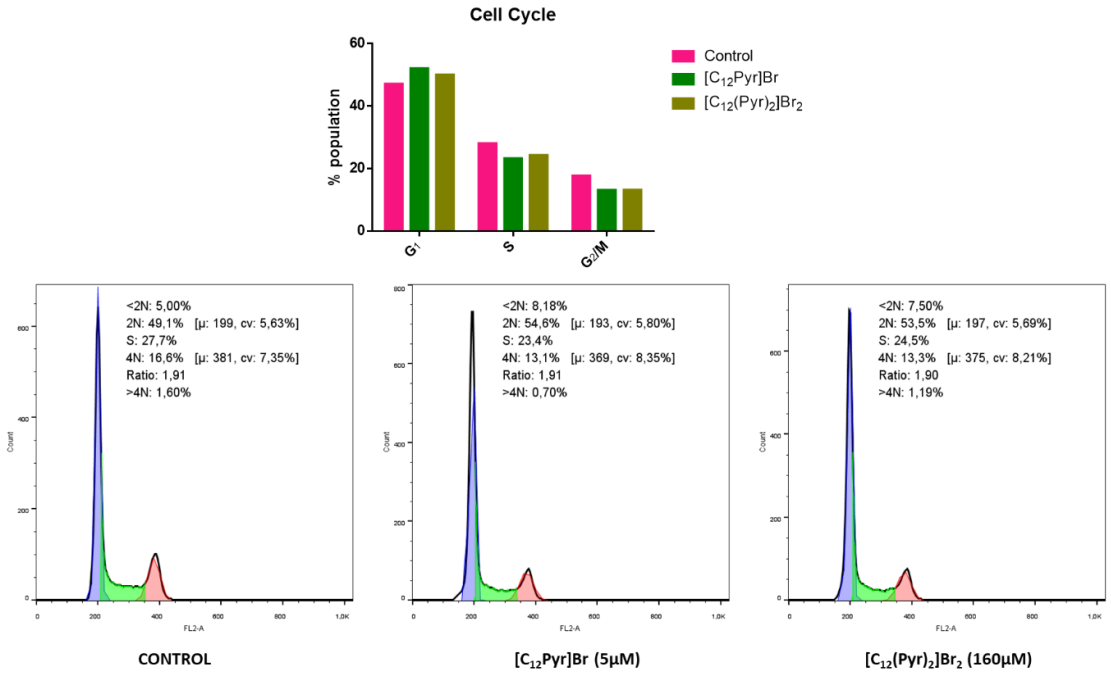

Figure 6. The cell cycle of HeLa cells exposed to different concentrations of $[C_{12}Pyr]Br$ and $[C_{12}(Pyr)_2]Br_2$ for 24 hours. HeLa cells not treated with IL were used as control.

3.3. Nuclear morphology in HeLa cells after being exposed to $[C_{12}Pyr]Br$

Observing cellular morphology is useful for distinguishing between apoptosis and necrosis during cell death. The nucleus fluorescence of HeLa cells after different exposure times (0, 30, 60 and 90 min) at a concentration of 8 μM of $[C_{12}Pyr]Br$, the most toxic IL in this work, can be found in Figure 7. The quantitative analysis showed that the fluorescence remained constant up to 60 min of exposure. Only at 90 min was an increase in nucleus fluorescence observed, due to the alteration in nucleus morphology occurred. Cell nuclei increased in size, perhaps due to the significant G1 phase arrest of cell cycle progression. This provides an opportunity for cells to either undergo repair mechanisms or follow the apoptotic pathway (Murad et al., 2016). According to Huber and Gerace (2007) and Jorgensen et al. (2007), a critical nucleus size is required for progression between the G1 and S phases in eukaryotic cells. However, in this case, cell nuclei did not reach a critical size to progress to the S phase as shown in Figures 5 and 6. Therefore, we infer that $[C_{12}Pyr]Br$ at a concentration of 8 μM after 90 min of treatment induces apoptosis in HeLa cells. These results agree with our MTT and flow cytometry results.

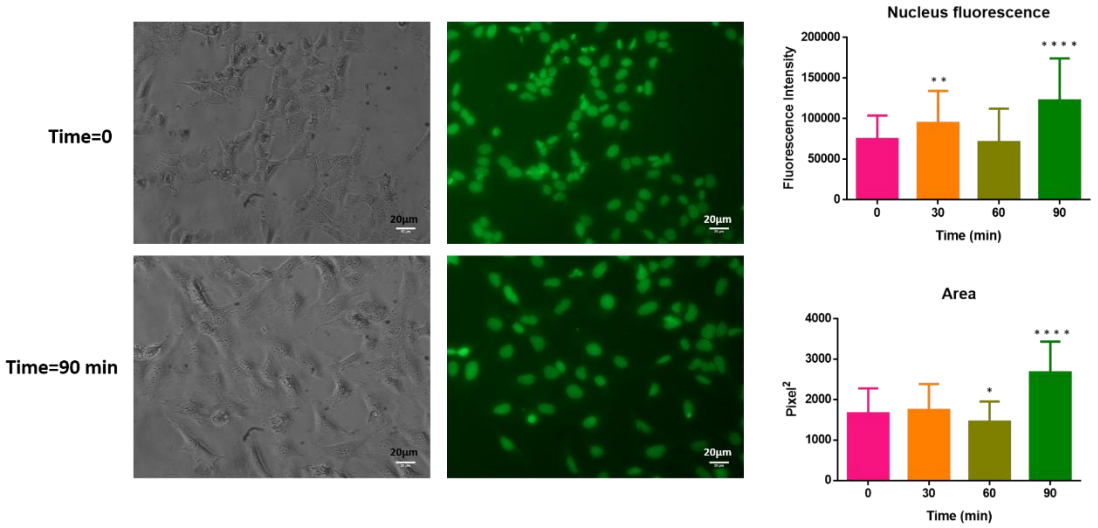

Figure 7. Nuclear morphology in HeLa cells induced by [C_{12}Pyr]Br at a concentration of 8 μM over 0, 30, 60 and 90 min using acridine orange staining. HeLa images correspond to the initial time and 90 min of treatment.

4. Conclusions

Some trends can be identified for the twelve monocationic and dicationic pyridinium-based ILs studied in this work. These are related to both their structural features and the cell line chosen to test their cytotoxicity. The results suggest that the cytotoxicity of the studied ILs on the four cell lines is highly dependent on their structure. The development of dicationic ILs, with a broad range of potential applications, but with lower cytotoxicity than their monocationic counterparts, can be considered in the sustainable design of new ILs for specific applications. The present results confirm that the mechanism of cell death followed by the most toxic IL used in this study, [C_{12}Pyr]Br, on HeLa cells was apoptotic. In addition, this work increases our knowledge of the cytotoxicity of pyridinium-based ILs, helping to amend the gap in the literature in this respect.

Acknowledgements

This work was partially supported by the European Commission (FEDER/ERDF) and the Spanish MINECO (Ref. CTQ2017-87708-R) and the research support programme of the Seneca Foundation of Science and Technology of Murcia, Spain (Ref. 20977/PI/18). M. G. Montalbán acknowledges support from MINECO (Juan de la Cierva-Formación contract, Ref. FJCI-2016-28081), P. Licence acknowledges EPSRC and BBSRC for support (EP/S005080/1, EP/P013341/1, BB/L013940/1).

References

Alvarez-Guerra, M., Irabien, A., 2011. Design of ionic liquids: an ecotoxicity (*Vibrio fischeri*) discrimination approach. Green Chem. 13, 1507-1516. https://doi.org/10.1039/c0gc00921k

Balducci, A., 2017. Ionic Liquids in Lithium-Ion Batteries. Top. Curr. Chem. 375, 20. https://doi.org/10.1007/s41061-017-0109-8

Chen, T.R., 1976. Microscopic demonstration of mycoplasma contamination in cell cultures and

391 cell culture media. Tissue Cult. Assoc. Man. 1, 229–232.
392 https://doi.org/10.1007/BF00917008

393 De Los Ríos, A.P., Hernández-Fernández, F.J., Martínez, F.A., Rubio, M., Víllora, G., 2007. The
394 effect of ionic liquid media on activity, selectivity and stability of *Candida antarctica* lipase
395 B in transesterification reactions. Biocatal. Biotransformation 25, 151–156.
396 https://doi.org/10.1080/10242420701379213

397 Denizalti, S., Ali, A.K., Ela, Ç., Ekmekci, M., Erten-Ela, S., 2018. Dye-sensitized solar cells using
398 ionic liquids as redox mediator. Chem. Phys. Lett. 691, 373–378.
399 https://doi.org/10.1016/J.CPLETT.2017.11.035

400 Diaz, E., Monsalvo, V.M., Lopez, J., Mena, I.F., Palomar, J., Rodriguez, J.J., Mohedano, A.F.,
401 2018. Assessment the ecotoxicity and inhibition of imidazolium ionic liquids by respiration
402 inhibition assays. Ecotoxicol. Environ. Saf. 162, 29–34.
403 https://doi.org/https://doi.org/10.1016/j.ecoenv.2018.06.057

404 e Silva, F.A., Siopa, F., Figueiredo, B.F.H.T., Gonçalves, A.M.M., Pereira, J.L., Gonçalves, F.,
405 Coutinho, J.A.P., Afonso, C.A.M., Ventura, S.P.M., 2014. Sustainable design for
406 environment-friendly mono and dicationic cholinium-based ionic liquids. Ecotoxicol.
407 Environ. Saf. 108, 302–310. https://doi.org/10.1016/j.ecoenv.2014.07.003

408 Earle, M.J., Seddon, K.R., 2002. Ionic Liquids: Green Solvents for the Future. Pure Appl. Chem.
409 72, 10–25. https://doi.org/10.1021/bk-2002-0819.ch002

410 Egorova, K.S., Gordeev, E.G., Ananikov, V.P., 2017. Biological Activity of Ionic Liquids and
411 Their Application in Pharmaceutics and Medicine. Chem. Rev. 117, 7132-7189.
412 https://doi.org/10.1021/acs.chemrev.6b00562

413 Gal, N., Malferarri, D., Kolusheva, S., Galletti, P., Tagliavini, E., Jelinek, R., Jelinek, R., 2012.
414 Membrane interactions of ionic liquids: Possible determinants for biological activity and
415 toxicity. Biochim. Biophys. Acta - Biomembr. 1818, 2967–2974.
416 https://doi.org/10.1016/j.bbamem.2012.07.025

417 Gindri, I.M., Siddiqui, D.A., Bhardwaj, P., Rodriguez, L.C., Palmer, K.L., Frizzo, C.P., Martins,
418 M.A.P., Rodrigues, D.C., 2014. Dicationic imidazolium-based ionic liquids: a new strategy
419 for non-toxic and antimicrobial materials. RSC Adv. 4, 62594–62602.
420 https://doi.org/10.1039/C4RA09906K

421 Gómez-Herrero, E., Tobajas, M., Polo, A., Rodriguez, J.J., Mohedano, A.F., 2018. Removal of
422 imidazolium- and pyridinium-based ionic liquids by Fenton oxidation. Environ. Sci. Pollut.
423 R. 25, 34930-34937. https://doi.org/10.1007/s11356-017-0867-4

424 Han, X., Armstrong, D.W., 2005. Using Geminal Dicationic Ionic Liquids as Solvents for High-
425 Temperature Organic Reactions. Org. Lett. 7, 4205–4208.
426 https://doi.org/10.1021/ol051637w

427 Hernández-Fernández, F.J., de los Ríos, A.P., Tomás-Alonso, F., Gómez, D., Rubio, M., Víllora,
428 G., 2007. Integrated reaction/separation processes for the kinetic resolution of *rac*-1-
429 phenylethanol using supported liquid membranes based on ionic liquids. Chem. Eng.
430 Process. Process Intensif. 46, 818–824.
431 https://doi.org/https://doi.org/10.1016/j.cep.2007.05.014

432 Hernández-Fernández, F.J., de los Ríos, A.P., Tomás-Alonso, F., Gómez, D., Víllora, G., 2008.
433 On the development of an integrated membrane process with ionic liquids for the kinetic
434 resolution of *rac*-2-pentanol. J. Memb. Sci. 314, 238–246.
435 https://doi.org/10.1016/j.memsci.2008.01.043

436 Huber, M.D., Gerace, L., 2007. The size-wise nucleus: Nuclear volume control in eukaryotes. J.
437 Cell Biol. 179, 583–584. https://doi.org/10.1083/jcb.200710156

438 Huddleston, J.G., Visser, A.E., Reichert, W.M., Willauer, H.D., Broker, G.A., Rogers, R.D.,
439 2001. Characterization and comparison of hydrophilic and hydrophobic room temperature
440 ionic liquids incorporating the imidazolium cation. Green Chem. 3, 156–164.
441 https://doi.org/10.1039/b103275p

442 Jin, C.-M., Ye, C., Phillips, B.S., Zabinski, J.S., Liu, X., Liu, W., Shreeve, J.M., 2006.
443 Polyethylene glycol functionalized dicationic ionic liquids with alkyl or polyfluoroalkyl
444 substituents as high temperature lubricants. J. Mater. Chem. 16, 1529-1535.
445 https://doi.org/10.1039/b517888f

446 Jorgensen, P., Edgington, N.P., Schneider, B.L., Rupes, I., Tyers, M., Futcher, B., 2007. The size
447 of the nucleus increases as yeast cells grow. Mol. Biol. Cell 18, 3523–3532.
448 https://doi.org/10.1091/mbc.e06-10-0973

449 Kumar, R.A., Papaı, N., Lee, J., Salminen, J., Clark, D.S., Prausnitz, J.M., 2008. In Vitro
450 Cytotoxicities of Ionic Liquids: Effect of Cation Rings, Functional Groups, and Anions.
451 Environ. Toxicol. 24, 388–395. https://doi.org/10.1002/tox

452 Lee, B.-S., Lin, S.-T., 2014. A priori prediction of the octanol–water partition coefficient (Kow)
453 of ionic liquids. Fluid Phase Equilib. 363, 233–238.
454 https://doi.org/10.1016/j.fluid.2013.11.042

455 Li, X.-Y., Jing, C.-Q., Lei, W.-L., Li, J., Wang, J.-J., 2012. Apoptosis caused by imidazolium-
456 based ionic liquids in PC12 cells. Ecotoxicol. Environ. Saf. 83, 102–107.
457 https://doi.org/10.1016/J.ECOENV.2012.06.013

458 Lozano-Pérez, A.A., Montalbán, M.G., Aznar-Cervantes, S.D., Cragnolini, F., Cenis, J.L.,
459 Víllora, G., 2015. Production of silk fibroin nanoparticles using ionic liquids and high-power
460 ultrasounds. J. Appl. Polym. Sci. 132. https://doi.org/10.1002/app.41702

461 Mahkam, M., Abbaszad Rafi, A., Mohammadzadeh Gheshlaghi, L., 2016. Preparation of novel
462 pH-sensitive nanocomposites based on ionic-liquid modified montmorillonite for colon
463 specific drug delivery system. Polym. Compos. 37, 182–187.
464 https://doi.org/10.1002/pc.23169

465 McLaughlin, M., Earle, M.J., Gîlea, M.A., Gilmore, B.F., Gorman, S.P., Seddon, K.R., 2011.
466 Cytotoxicity of 1-alkylquinolinium bromide ionic liquids in murine fibroblast NIH 3T3
467 cells. Green Chem. 13, 2794–2800. https://doi.org/10.1039/C0GC00813C

468 Miwa, Y., Hamamoto, H., Ishida, T., 2016. Lidocaine self-sacrificially improves the skin
469 permeation of the acidic and poorly water-soluble drug etodolac via its transformation into
470 an ionic liquid. Eur. J. Pharm. Biopharm. 102, 92–100.
471 https://doi.org/https://doi.org/10.1016/j.ejpb.2016.03.003

472 Mizuuchi, H., Jaitely, V., Murdan, S., Florence, A.T., 2008. Room temperature ionic liquids and
473 their mixtures: Potential pharmaceutical solvents. Eur. J. Pharm. Sci. 33, 326–331.
474 https://doi.org/https://doi.org/10.1016/j.ejps.2008.01.002

475 Moniruzzaman, M., Kamiya, N., Goto, M., 2010. Ionic liquid based microemulsion with
476 pharmaceutically accepted components: Formulation and potential applications. J. Colloid
477 Interface Sci. 352, 136–142. https://doi.org/https://doi.org/10.1016/j.jcis.2010.08.035

478 Montalbán, M.G., Bolívar, C.L., Díaz Baños, F.G., Víllora, G., 2015. Effect of Temperature,
479 Anion, and Alkyl Chain Length on the Density and Refractive Index of 1-Alkyl-3-
480 methylimidazolium-Based Ionic Liquids. J. Chem. Eng. Data 60, 1986-1996.

https://doi.org/10.1021/je501091q

Montalbán, M.G., Collado-González, M., Lozano-Pérez, A.A., Díaz Baños, F.G., Víllora, G., 2018a. Extraction of organic compounds involved in the kinetic resolution of *rac*-2-pentanol from *n*-hexane by imidazolium-based ionic liquids: Liquid-liquid equilibrium. J. Mol. Liq. 252,445-453. https://doi.org/10.1016/j.molliq.2017.12.157

Montalbán, M.G., Trigo, R., Collado-González, M., Díaz-Baños, F.G., Víllora, G., 2016a. Liquid-liquid equilibria for ternary mixtures of 1-alkyl-3-methyl imidazolium bis{(trifluoromethyl)sulfonyl}imides, *n*-hexane and organic compounds at 303.15K and 0.1MPa. J. Chem. Thermodyn. 103, 403–413. https://doi.org/10.1016/j.jct.2016.08.033

Montalbán, M.G., Hidalgo, J.M., Collado-González, M., Díaz Baños, F.G., Víllora, G., 2016b. Assessing chemical toxicity of ionic liquids on *Vibrio fischeri*: Correlation with structure and composition. Chemosphere 155, 405–414. https://doi.org/10.1016/j.chemosphere.2016.04.042

Montalbán, M.G., Víllora, G., Licence, P., 2018b. Ecotoxicity assessment of dicationic *versus* monocationic ionic liquids as a more environmentally friendly alternative. Ecotoxicol. Environ. Saf. 150, 129-135. https://doi.org/10.1016/j.ecoenv.2017.11.073

Montalbán, M.G., Víllora, G., Licence, P., 2018c. Synthesis and characterization data of monocationic and dicationic ionic liquids or molten salts. Data Br. 19, 769–788. https://doi.org/10.1016/j.dib.2018.05.080

Murad, H., Hawat, M., Ekhtiar, A., AlJapawe, A., Abbas, A., Darwish, H., Sbenati, O., Ghannam, A., 2016. Induction of G1-phase cell cycle arrest and apoptosis pathway in MDA-MB-231 human breast cancer cells by sulfated polysaccharide extracted from Laurencia papillosa. Cancer Cell Int. 16, 1–11. https://doi.org/10.1186/s12935-016-0315-4

Qi, M., Armstrong, D.W., 2007. Dicationic ionic liquid stationary phase for GC-MS analysis of volatile compounds in herbal plants. Anal. Bioanal. Chem. 388, 889–899. https://doi.org/10.1007/s00216-007-1290-3

Ranke, J., Mölter, K., Stock, F., Bottin-Weber, U., Poczobutt, J., Hoffmann, J., Ondruschka, B., Filser, J., Jastorff, B., 2004. Biological effects of imidazolium ionic liquids with varying chain lengths in acute Vibrio fischeri and WST-1 cell viability assays. Ecotoxicol. Environ. Saf. 58, 396–404. https://doi.org/10.1016/S0147-6513(03)00105-2

Romero, D., Gómez-Zapata, M., Luna, A., García-Fernández, A., 2004. Comparison of cytopathological changes induced by mercury chloride exposure in renal cell lines (VERO and BGM). Environ. Toxicol. Pharmacol. 17, 129–141. https://doi.org/10.1016/J.ETAP.2004.03.007

Salminen, J., Papaiconomou, N., Kumar, R.A., Lee, J.-M., Kerr, J., Newman, J., Prausnitz, J.M., 2007. Physicochemical properties and toxicities of hydrophobic piperidinium and pyrrolidinium ionic liquids. Fluid Phase Equilibr. 261, 421–426. https://doi.org/10.1016/j.fluid.2007.06.031

Stepnowski, P., Skladanowski, A.C., Ludwiczak, A., Laczyn, E., 2004. Evaluating the cytotoxicity of ionic liquids using human cell line HeLa. Hum. Exp. Toxicol. 23, 513–517. https://doi.org/10.1191/0960327104ht480oa

Steudte, S., Bemowsky, S., Mahrova, M., Bottin-Weber, U., Tojo-Suarez, E., Stepnowski, P., Stolte, S., 2014. Toxicity and biodegradability of dicationic ionic liquids. RSC Adv. 4, 5198-5205. https://doi.org/10.1039/c3ra45675g

Thamke, V.R., Chaudhari, A.U., Tapase, S.R., Paul, D., Kodam, K.M., 2019. In vitro

toxicological evaluation of ionic liquids and development of effective bioremediation process for their removal. Environ. Pollut. 250, 567–577. https://doi.org/10.1016/J.ENVPOL.2019.04.043

Ventura, S.P.M., Marques, C.S., Rosatella, A.A., Afonso, C.A.M., Gonçalves, F., Coutinho, J.A.P., 2012. Toxicity assessment of various ionic liquid families towards Vibrio fischeri marine bacteria. Ecotoxicol. Environ. Saf. 76, 162–168. https://doi.org/10.1016/j.ecoenv.2011.10.006

Vieira, N.S.M., Bastos, J.C., Rebelo, L.P.N., Matias, A., Araújo, J.M.M., Pereiro, A.B., 2019. Human cytotoxicity and octanol/water partition coefficients of fluorinated ionic liquids. Chemosphere 216, 576–586. https://doi.org/https://doi.org/10.1016/j.chemosphere.2018.10.159

Viswanathan, G., Murugesan, S., Pushparaj, V., Nalamasu, O., Ajayan, P.M., Linhardt, R.J., 2006. Preparation of Biopolymer Fibers by Electrospinning from Room Temperature Ionic Liquids. Biomacromolecules 7, 415–418. https://doi.org/10.1021/bm050837s

Welton, T., 2004. Ionic liquids in catalysis. Coord. Chem. Rev. 248, 2459–2477. https://doi.org/10.1016/J.CCR.2004.04.015

Wu, S., Zeng, L., Wang, C., Yang, Y., Zhou, W., Li, F., Tan, Z., 2018. Assessment of the cytotoxicity of ionic liquids on Spodoptera frugiperda 9 (Sf-9) cell lines via in vitro assays. J. Hazard. Mater. 348, 1–9. https://doi.org/10.1016/j.jhazmat.2018.01.028

Xia, X., Wan, R., Wang, P., Huo, W., Dong, H., Du, Q., 2018. Toxicity of imidazoles ionic liquid [C16mim]Cl to Hela cells. Ecotoxicol. Environ. Saf. 162, 408–414. https://doi.org/https://doi.org/10.1016/j.ecoenv.2018.07.022